COMPOSITE BEAM-COLUMNS PERFORMANCE BASED ON NONLINEAR FIBER AND FINITE ELEMENT ANALYSIS

T. Perea[1] and R.T. Leon[2]

[1] *Ph.D. Candidate, Dept. of Civil and Structural Engineering, Georgia Institute of Technology. USA*
[2] *Professor, Dept. of Civil and Structural Engineering, Georgia Institute of Technology. USA*
Email: tperea@gatech.edu, roberto.leon@cee.gatech.edu

ABSTRACT:

Results obtained from nonlinear fiber analyses (FA) and finite element analyses (FEA) for concrete-filled-tubes (CFT) are discussed. These analyses, based on the assumed stress-strain material curves, member slenderness, initial imperfections, and material and geometric nonlinearities, etc., were aimed at assessing primarily the overall behavior on these structural elements as a prelude to a large full-scale testing program. Some results are compared with those obtained from AISC (2005) or analytical equations published in the literature. Fiber and finite based results show a compatible correlation with the expected element behavior, which is also captured in the current 2005 AISC Specifications and 2005 AISC Seismic Provisions.

KEYWORDS: CFT, Concrete Filled Tube, Composite, Beam-Column, Fiber, Finite, AISC

1. INTRODUCTION

Fiber Element Analysis is a numerical technique which models a structural element by dividing it into a number of two-end frame elements, and by linking each boundary to a discrete cross-section with a grid of fibers. The material stress-strain response in each fiber is integrated to get stress-resultant forces and rigidity terms, and from these, forces and rigidities over the length are obtained through finite element interpolation functions which must satisfy equilibrium and compatibility conditions.

There are several advantages which justify the use of fiber analysis. Some of these advantages include but are not limited to their ability to handle:

- Complex cross-sections: A fiber cross-section can have any general geometric configuration formed by subregions of simpler shapes; geometric properties are calculated through the numerical integration.
- Tapered elements: Since the length of the fiber is not considered, the cross-section defined at each of the two ends can be different, and therefore, the response can be roughly estimated. Precision can be increased with more integration points.
- Complex strength-strain behavior: Since each fiber can have any stress-strain response, this technique allows modeling nonlinear behavior in steel members, reinforced concrete members (unconfined and confined concrete σ–ε), and composite members.
- Accuracy and efficiency: Since each fiber is associated to a given uniaxial stress-strain (σ–ε) material response, higher accuracy and more realistic behavior effects can be captured in a fiber-based model than in a frame-based model, and at less computing time than for a 3D finite-based model.

As described previously, the uniaxial σ–ε curve can directly account for the material nonlinearity in monotonic or cyclic loads or displacements, and the residual stresses in the structural steel members. However, some researchers have calibrated, based on experimental or analytical 3D finite-based results (i.e. Varma et al., 2004; Tort and Hajjar, 2007), the uniaxial σ–ε to account for additional behavior effects like:

- Confinement effects in the concrete due to either steel reinforcement (as in RC or SRC cross-sections) or a steel tube (as in CFT cross-sections). Concrete confinement in CFT elements remain while the steel-concrete contact is hold.

- Local buckling in steel tubes through a degradation of the compressive σ–ε beyond the corresponding strain (ε_{lb}). Local buckling in CFT elements can be reached when the steel, with relatively low width-to-thickness ratio, is highly stressed in compression and the steel-concrete contact is lost.

Stability effects through geometric nonlinearity and initial imperfections can be captured directly with the frame-based analysis. In turn, slip between concrete and steel have been modeled in the frame-based formulation by adding degrees-of-freedom (i.e. Hajjar et al., 1998, Aval et al., 2002; Tort and Hajjar, 2007).

On the other hand, Finite Element Analysis (FEA) is a numerical technique which models a structural system by a set of appropriate finite elements (1D, 2D or 3D) interconnected at the exterior nodes, and all together covers the entire system as accurate as possible. Nodes will have the desired degrees of freedom which may include translations, rotations, and for special applications, higher order derivatives of displacements. When the nodes displace, they will drag the elements along in a certain manner dictated by the element formulation, so the displacements of any points in the element will be interpolated from the nodal displacements through the finite element interpolation or shape functions, which must satisfy equilibrium and compatibility conditions as well.

There are several advantages which justify the use of finite element analysis. Some of these advantages include but are not limited to their ability to handle:

- Complex 3D geometries: 1D, 2D or 3D elements may be used to generate any 2D or 3D shape of any structural system.
- True material non-linearity: Since the analysis account for size and shape changes, true stress-strain "σ–ε" values are used in the calculations instead of the engineering stress-strain (s-e) values.
- Geometric nonlinearity and initial conditions (like residuals stress or strains, out-of-plumbness, out-of straightness, etc.) may be included in the model.
- Definition of surfaces in contact allows having a better understanding of the true steel-concrete interaction. In composite columns, for example, the normal and tangential contact interaction between the steel and concrete's surfaces may allowed to account directly for effects which in fiber analysis are indirectly implicit in the uniaxial σ–ε. Thus, as long as the steel-concrete remain in contact, neither local buckling, lost of confinement, nor slip take place. Accounting for contact in finite element analysis may include but are not limited to their ability to handle:
  - Confinement directly provided by the normal pressure between the surfaces in contact; modification in the uniaxial σ–ε curve is not needed.
  - Local buckling of the steel tube is delayed until loss of normal contact takes place.
  - Slip or unbonding in concrete-steel surfaces takes place when tangential contact is lost.
  - Wear can be predicted in mechanical parts with friction or relative motion between contact surfaces, mainly when these are subjected to high cycle fatigue.

Since the model may have a large amount of elements, computing time or resources are an important issue to consider; in order to obtain a good accuracy without excessive processing, the following is often recommended.

- Symmetry or anti-symmetry conditions are exploited in order to reduce the size of the system. Compatibility of displacements of many nodes can be imposed via constraint relations; proper support constraints are imposed with special attention paid to nodes on symmetry axes.
- The element mesh should be fine enough in order to have acceptable accuracy. To assess accuracy, the mesh is refined until results show little change. For higher accuracy, the elements' aspect ratio should be as close to unity as possible and smaller elements can be used over the parts of higher stress gradient.

2. DISCUSSION AND ANALYSIS

Nonlinear analyses are obviously sensitive to the assumptions in the stress-strain curves. Consequently, several research studies have been conducted on this topic to predict more "realistic" responses.

The current AISC (2005) specification allows the use of fully-plastic stress distribution and strain compatibility methods to calculate the cross-section strength. The plastic distribution method (Roik and Bergmann, 1992) basically assumes that each component in cross-section has reached the maximum plastic stress (Figure 1). The assumed plastic stress in circular CFTs ($0.95f_c$') is higher than the one assumed in rectangular CFTs or SRCs ($0.85f_c$') to account in some fashion for a higher confinement in the circular tubes.

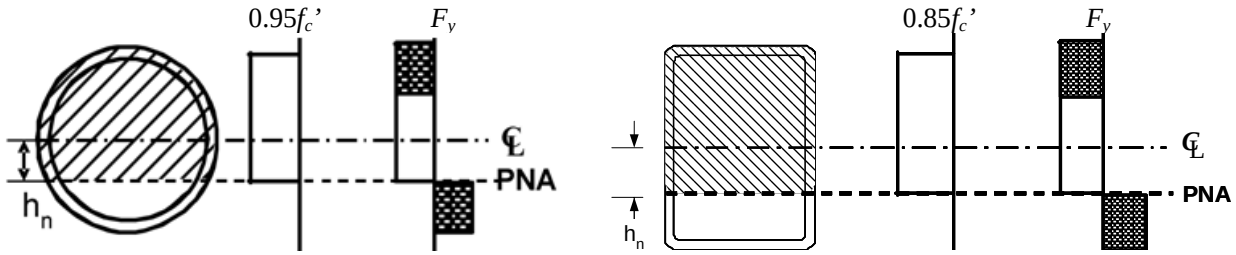

a) Encased SRC b) Rectangular CFT

Figure 1. Fully-plastic stress distribution in composite cross-sections

While very useful and accurate for design purposes, the plastic distribution approach can only match the ultimate strength of the cross-section. When the entire moment-curvature (or load-deformation) behavior is of interests, more complex uniaxial stress-strain curves are needed. These include strain compatibility approaches to model reinforced concrete elements (i.e. Kent and Park, 1973; Mander et. al., 1988), steel members (i.e. Menegotto and Pinto, 1973), concrete filled tubes (CFT) elements (i.e. Collins and Mitchell, 1990; Sakino and Sun, 1994; Chang and Mander, 1994; Nakahara and Sakino, 1998; Susantha et al., 2001), and steel-reinforced-concrete (SRC) members (similar to those used for RC and steel).

The behavior of concrete under triaxial stresses was originally studied by Richart et al. in 1928 (Park and Paulay, 1975). They observed that strength and ductility of concrete are improved under triaxial compression, and based on their experimental results, they proposed the following equations.

$$f_{cc}' = f_c' + k \cdot \sigma_r$$
$$\varepsilon_{cc} = \varepsilon_c \left(1 + 5k\sigma_r / f_c'\right) \quad (1)$$

Where f_{cc}' and ε_{cc} are the confined strength and strain, respectively. f_c' and ε_c are the unconfined strength and strain, respectively. σ_r is the confining pressure, and k is a confining coefficient defined with the value of 4.1 originally by Richart et al. in 1928 (Park and Paulay, 1975). Based on experimental results, an average confining coefficient of k=5.6 with values between 4.5 and 7.0, was obtained by Balmer in 1949 (Park and Paulay, 1975).

Confining pressure or hoop stresses (σ_r) on circular RC columns can be calculated by the equation below (Park and Paulay, 1975), which assumes yielding limit state of the spiral steel.

$$\sigma_r = \frac{2F_y A_{sp}}{D \cdot s} \quad (2.a)$$

Where D is, for this case, the diameter of the confined concrete section; s and A_{sp} are the spacing and area of the steel spirals or hoops, respectively. Note that the steel are mainly subjected under uniaxial stress ($\sigma_\theta = F_y$).

Adapting the last equation in circular CFT cross-sections, assuming yielding limit state of the steel tube, the confining pressure in the tube under biaxial stresses is given by:

$$\sigma_r = \frac{2\alpha F_y t}{D-2t} \tag{2.b}$$

Where D, t, L are, respectively, the outer diameter, thickness and length of the circular steel tube. F_y is the yield stress of the steel, and α is the tangential-to-axial stress ratio (σ_θ/F_y), which depends on the axial force and the D/t ratio. Note that, in this case, the tube is mainly subjected under biaxial stress ($\sigma_\theta=\alpha F_y$ and $\sigma_z=\beta F_y$).

From experimental data, Sakino and Sun calibrated the α (σ_θ/F_y) and β (σ_z/F_y) values, and assuming Von-Mises failure criteria and other assumptions these came up with α=0.19 and $\beta_{compression}$=0.89, $\beta_{tension}$=1.08. The β values are also used in the σ–ε of the steel tube to account for biaxial stresses (Figure 3). Thus, based on empirical data and its calibration with an analytical study, Sakino and Sun (1994) proposed uniaxial σ–ε models for both concrete (Equation 3, Figure 2) and steel (Figure 3) for circular and rectangular CFT elements that account for confinement, local buckling and biaxial stresses. Equation 3 describes the σ–ε curve for concrete proposed by Sakino and Sun (1994), which is in terms of the effective hoop stresses (σ_{re}) and the peak concrete strength.

$$\sigma(\varepsilon) = f_{cc}'\left(\frac{V(\varepsilon/\varepsilon_{cc})+(W-1)(\varepsilon/\varepsilon_{cc})^2}{1+(V-2)(\varepsilon/\varepsilon_{cc})+W(\varepsilon/\varepsilon_{cc})^2}\right) \tag{3}$$

Where: $V = \frac{E_c\varepsilon_{cc}}{f_{cc}'}$ $W = 1.5 - 0.1179\, f_c'(ksi) + 1.3086\sqrt{\sigma_r(ksi)}$

And the hoop stresses (σ_r) and the peak strength values are defined by:

For circular CFTs

$$\sigma_r = \frac{0.38F_y}{D/t-2}$$

$$f_{cc}' = f_c' + \frac{1.558F_y}{D/t-2}$$

$$\varepsilon_{cc} = \begin{cases} \varepsilon_c\left[1+4.7\left(\frac{f_{cc}'}{f_c'}-1\right)\right] & if \quad f_{cc}' < 1.5\, f_c' \\ \varepsilon_c\left[3.35+20\left(\frac{f_{cc}'}{f_c'}-1.5\right)\right] & if \quad f_{cc}' \geq 1.5\, f_c' \end{cases}$$

For rectangular CFTs

$$\sigma_r = \frac{2(b/t-1)F_y}{(b/t-2)^3}$$

$$f_{cc}' = f_c'$$

$$\varepsilon_{cc} = \varepsilon_c = 0.94x10^{-3}\left(f_c'(MPa)\right)^{0.25}$$

Figure 2 shows σ–ε curves obtained with the Sakino and Sun model in a 5 ksi strength concrete that is confined by circular and rectangular steel tubes with 50 and 100 width-to-thickness ratios (D/t, b/t). As shown in this figure, confinement improves strength and ductility in circular CFTs and just ductility in rectangular CFTs. This figure also shows a cyclic model (which was proposed by Karsan and Jirsa in 1969 and implemented in the OpenSees software) to account for unloading and reloading reversible loads.

In turn, steel tubes can be modeled through an unsymmetrical σ–ε curve to satisfy the Von Misses yield criteria with biaxial stresses. Depending on the b/t ratio, local buckling in rectangular tubes can be handled by a descending branch of the σ–ε curve at a critical strain (ε_{lb}). A careful calibration of the experimental data is needed to obtain the strain ε_{lb} when local buckling takes place. This model postulates that ε_{lb} in circular tubes is reached at high values of strain, and therefore, local buckling effects can be neglected; this approach is tied to the Japanese design requirements for b/t ratios which basically preclude this failure mode. The cyclic behavior illustrated in Figure 3 accounts for unloading and reloading reversible loads.

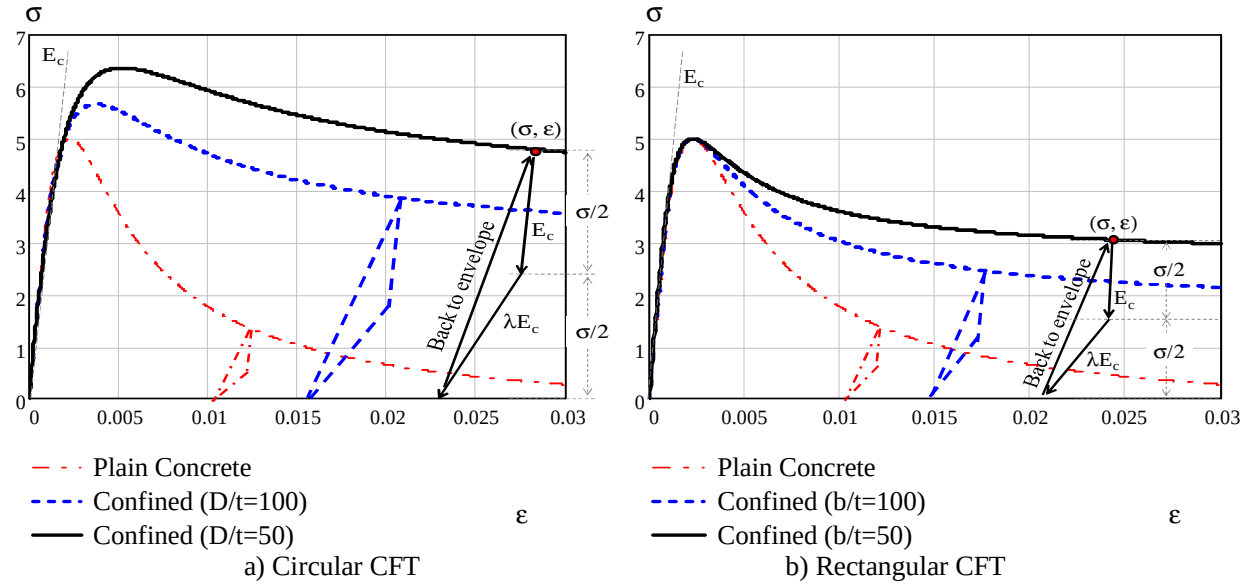

Figure 2. Stress-strain (σ–ε) curves obtained for a 5 ksi strength concrete confined by a steel tube with different width-to-thickness ratios; the cyclic unloading/reloading model is schematically illustrated.

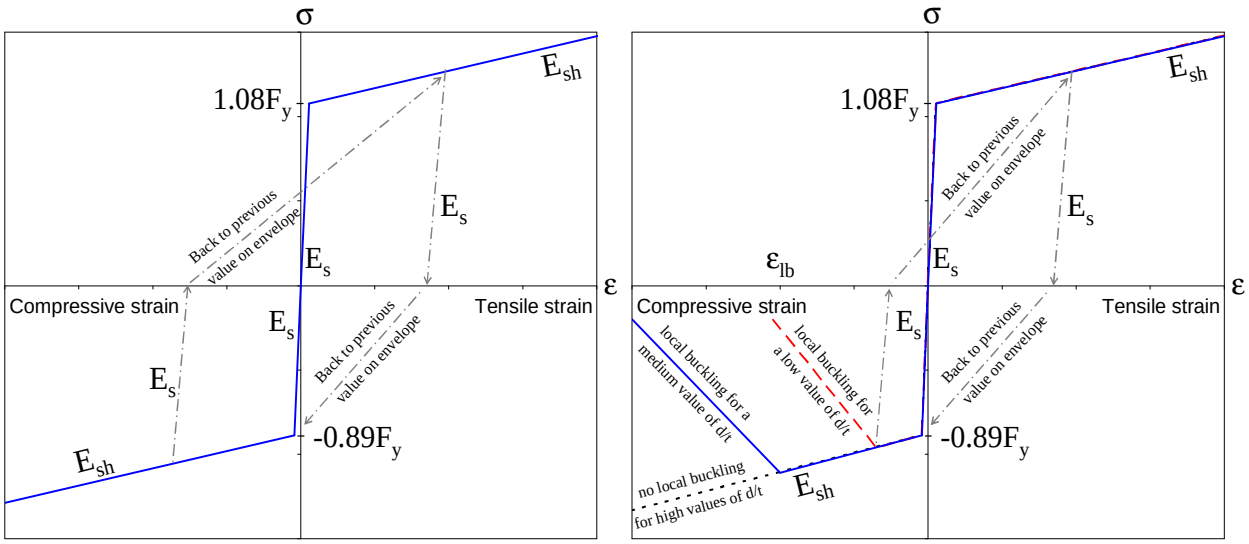

Figure 3. Stress-strain (σ–ε) curves for steel tubes in CFT beam-columns; cyclic unloading/reloading rules are schematically illustrated, as well as local buckling where applies.

In order to evaluate the effects of confinement in short columns, a cylinder of concrete filled into a steel tube was analyzed using the finite element method. The steel tube (F_y=42 ksi and D/t=240) is modeled by 20-join 3D solids (C3D20R), while the concrete (f_c' = 5 ksi, plain concrete σ–ε assumed) is integrated by 8-joint 3D-solids (C3D8R) and 6-joint wedges (C3D6). After assembling the CFT element (Figure 4.a), interaction of steel-concrete surfaces in contact was defined by the normal-hard contact model, which allows separation but avoid overclosure; a small adjustment zone was defined to avoid inaccuracy due to the numerical noise range. The concrete element was loaded in monotonic compression force (Figure 4.b.ii), while the tube has three preload cases: i) no preload in the steel tube ($\varepsilon_s=0$); ii) with a low preload compression in the steel tube such that the strain in the tube reach the yielding strain ($\varepsilon_s=\varepsilon_y=F_y/E_s$); iii) with a high preload compression in the steel tube such that the steel tube exceed 5 times the yielding strain ($\varepsilon_s=5\varepsilon_y$, Figure 4.b.i).

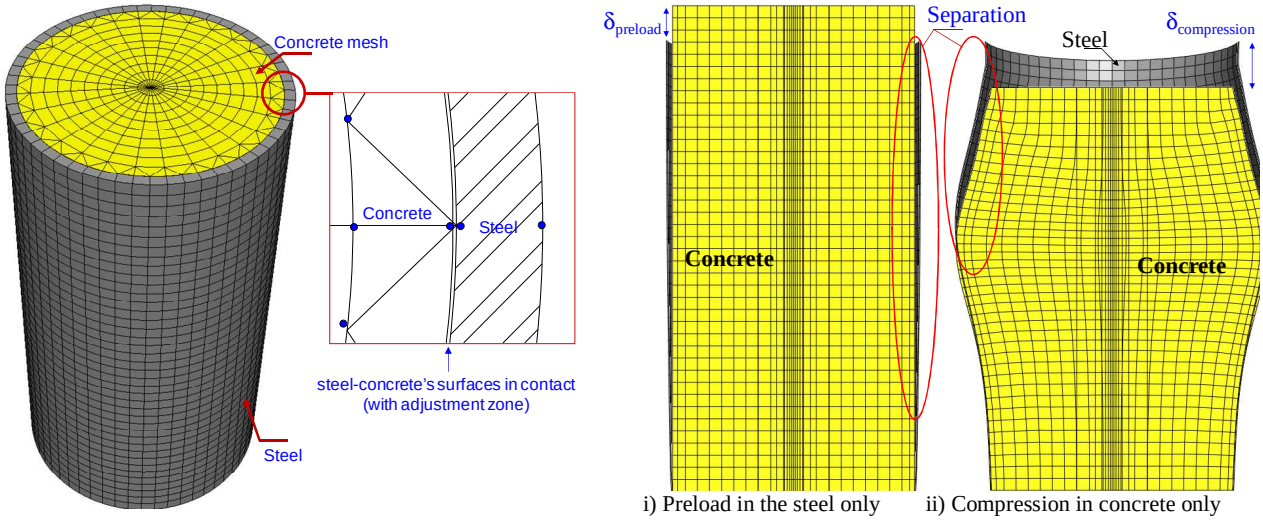

a) Finite element model b) displaced shape (10X amplification)

Figure 4. Finite element model of a CFT cylinder, and its displaced shape of the CFT with a preload in the steel tube followed by a compression force in the concrete

The results of the hoop stresses in the concrete confined by the steel tube, and the corresponding σ–ε for confined concrete proposed by Sakino and Sun (1994) are illustrated in Figure 5. As seen in Figure 5.a, the concrete-steel contact in the tube increases the hoop stresses as the compression force increments; as seen in Figure 4.b.i, the cases with an initial preload in the steel tube produces an initial separation (or a contact delay) which is eventually closed as the compression in the concrete make it expand and go back in contact; however, as soon as the steel and concrete surfaces are in contact, the σ–ε tends to go from the plain concrete curve to the confined concrete curve (Figure 5.b). Notice than maximum both hoop stresses and maximum confined strength from FEA are very close to those estimated with the empirical equations proposed by Richart (1928). Sakino and Sun prediction is very similar in strength and ductility to the σ–ε curve when the tube had a high preload.

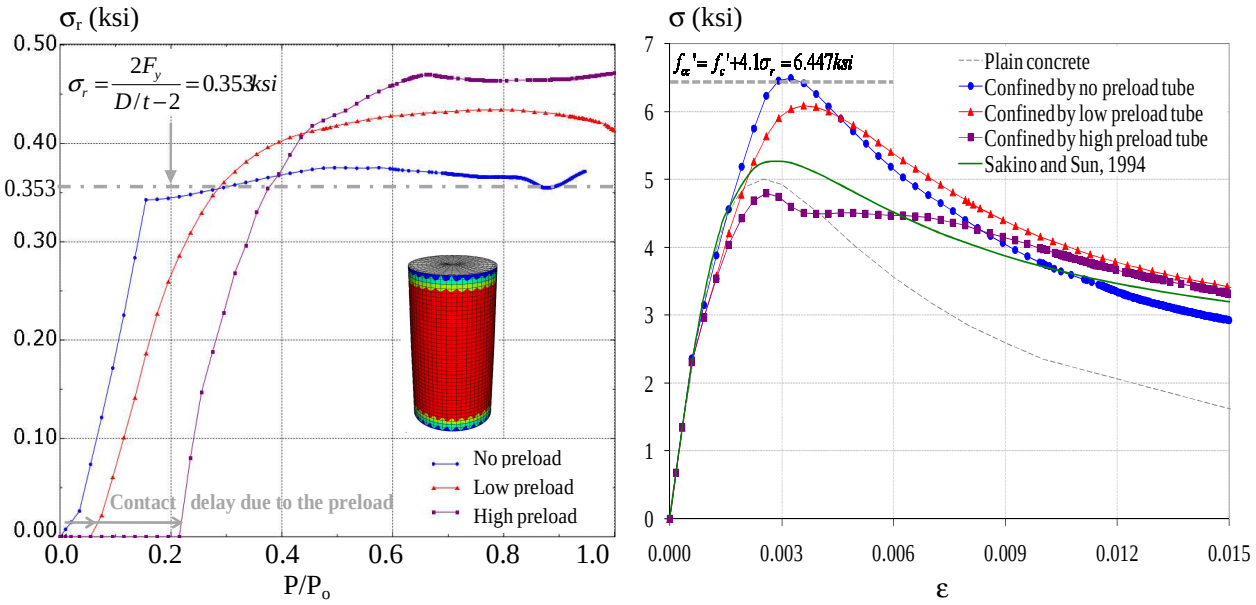

a) Hoop stress vs. Normalized compression b) Uniaxial stress-strain (σ–ε)

Figure 5. Variation of the hoop stresses with the compression force, and the uniaxial stress-strain (s-e) obtained from the finite element analysis.

Figure 6 shows results obtained from nonlinear fiber analysis for the prediction of a circular CFT beam-column integrated by an HSS20x0.25 steel tube (A500 Gr. B, D/t=86) filled with 5 ksi strength concrete. These results show envelopes of ultimate strength (as in the P-λ curves or in the P-M diagrams), and both strength and expected ductility when the element is subjected to lateral cyclic loads (as in the M-ϕ or F-Δ curves). Member slenderness, initial imperfections, and material and geometric nonlinearities were accounted in these analyses; confinement effects (through a modification in the concrete σ–ε curve as shown in Figure 2.a) and biaxial stresses (through the asymmetrical steel σ–ε curve as shown in Figure 3.a) are also implicit in these results. The cyclic models schematically shown in Figures 2.a and 3.a were taken into account when unloading and reloading cyclically.

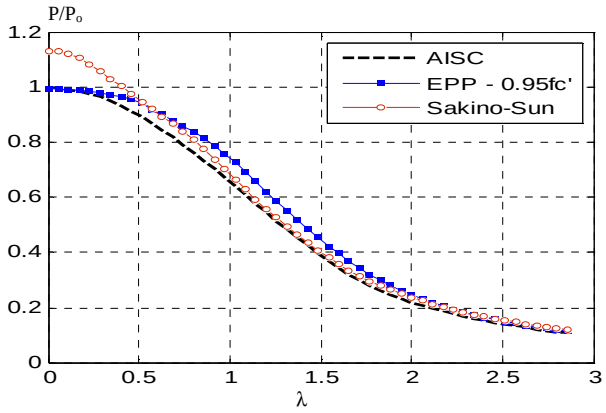

a) Moment-curvature

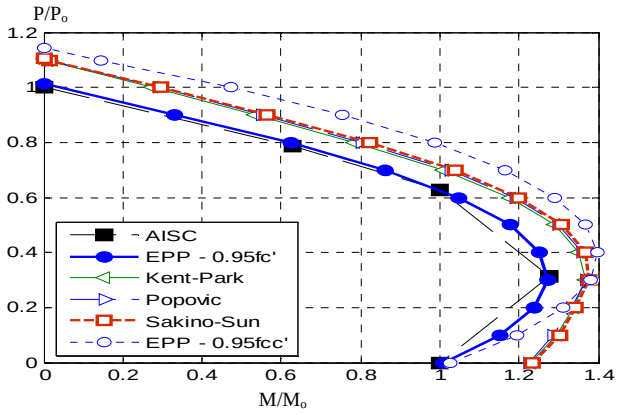

b) Column curve

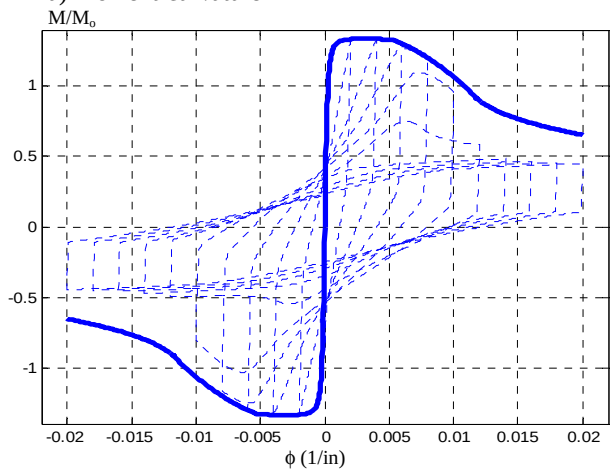

c) P-M interaction diagram, cross-section strength

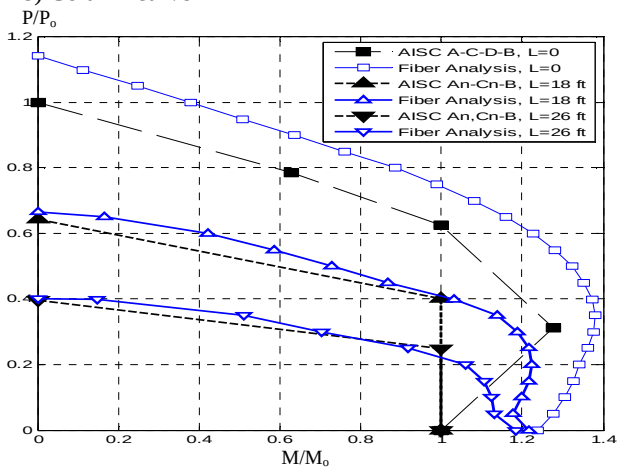

d) P-M interaction diagram, beam-column strength

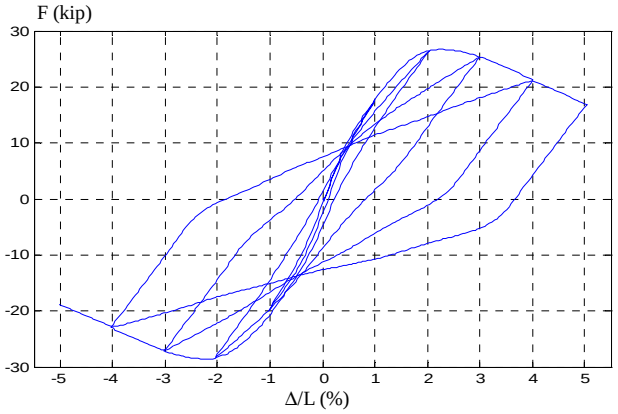

e) Force vs. Displacement, L=18 ft.

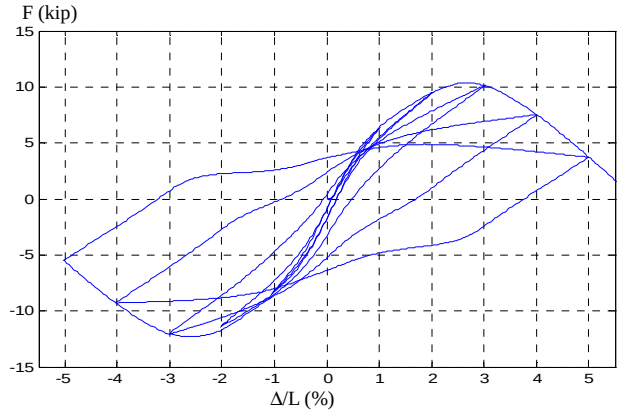

f) Force vs. Displacement, L=26 ft.

Figure 6. Results from fiber element analysis for a circular CFT column (D=20", t=0.25", F_y=42 ksi, f'_c=5 ksi)

CONCLUSIONS

The benefits on the fiber and finite element analysis technique were briefly described. Based on these techniques, some results were obtained and shown emphasizing some issues in the structural behavior of composite cross-sections and composite beam-column elements, such as the effects due to the compressive force, material nonlinearity (stress-strain model), concrete confinement, steel local buckling, triaxial stresses, initial imperfection and geometric nonlinearity effects. Fiber-based analytical results were also compared with those obtained with the AISC (2005) Specification.

As described previously, fiber and finite element analysis analyses are very useful techniques to predict the overall behavior of composite beam-column elements. However, the accuracy on the results is highly dependable on the stress-strain model coupled to the fibers or to the solids. Simple stress-strain models predict reasonably the ultimate strength; however, more complex material models should be assumed to predict ductility and high displacements such that damage is considered. On the other hand, most of the nonlinearity sources (like strength/stiffness degradation, confinement, local buckling and triaxial stresses effects) have to be calibrated with experimental results and/or more complex analytical techniques in order to incorporate them later on in the uniaxial stress-strain used in the fiber-based model.

3D finite element analysis can deal with these sources in a straightforward manner. Definition of contact surfaces between concrete and steel allows a more realistic interaction within these materials; therefore, confinement, local buckling and triaxial stresses can be directly integrated in the behavior (with no influence on the material model). More computing resources and time will be required though.

ACKNOWLEDGEMENT

The work described here is part of a NEESR project funded as NSF Grant 0619047. The opinions and conclusions are solely those of the authors and not those of the national Science Foundation

REFERENCES

AISC (2005), "*Specifications for structural steel buildings*". **ANSI/AISC 360-05**. Chicago, IL, USA.

AISC Seismic Manual (2005), "*Seismic Provisions for structural steel buildings*". **ANSI/AISC 341-05**. Chicago, IL.

Aval, S. Saadeghvaziri, M. and Golafshani, A. (2002). "Comprehensive composite inelastic fiber element for cyclic analysis of concrete-filled steel tube columns". *Journal of Engineering Mechanics*, **Vol. 128, No. 4**, ASCE, pp. 428-437.

Hajjar, J. Schiller, P. and Molodan, A. (1998). ''A distributed plasticity model for concrete-filled steel tube beam-columns with interlayer slip'' *Journal of Engineering Structures*, **Vol. 20, No. 8,** pp. 663–676.

Karsan, I. and Jirsa, J. (1969). "Behavior of concrete under compressive loading". *J. of Structural Division*, ASCE, **95-12**

Park, R. and Paulay, T. (1975). "*Reinforced concrete structures*". Wiley-Interscience. **ISBN 0-471-65917-7**. pp. 11-47.

Roik, K. and Bergmann, R. (1992), "*Composite columns*". Constructional steel design. Dowling, P. Harding, J. and Bjorhovde, R. (eds.). Elsevier Sc. Publ. **ISBN 1-85166-895-0.** New York. pp. 443–470.

Tort, C. and Hajjar, J. (2007). "*Reliability-based performance-based design of rectangular concrete-filled steel tube members and frames*". **Report No. ST-07-1**. University of Minnesota. Department of Civil Engineering. Minneapolis, MN.

Varma, A. Ricles, J. Sauce, R. and Wu Lu, L. (2004), "Seismic behavior and design of high-strength square concrete-filled steel tube beam columns". *Journal of Structural Engineering*. **Vol. 130, No. 2,** pp. 169-179.

Richart, F. Brandtzaeg, A. and Brown, R. (1929), "*The failure of plain and spirally reinforced concrete in compression*", **Report No. 190**. University of Illinois, Engineering Experimental Station.

Kent, D. and Park, R. (1973), "Flexural members with confined concrete", *J. of Structural Division*, ASCE, **Vol. 97, No. 7**.

Mander, J. Priestley, M. and Park, R. (1988), "Theoretical stress-strain model for confined concrete." *Journal of Structural Engineering*. ASCE, **Vol. 114, No. 8**. pp. 1804-1825.

Sakino, K. y Sun, Y. (1994), ''Stress–strain curve of concrete confined by rectangular hoop'', *Structural and Construction Engineering*, AIJ, **No. 461**, pp. 95–104.